ACS APPLIED MATERIALS & INTERFACES

Research Article

www.acsami.org

Double Perovskite Sr_2FeMoO_6 Films Prepared by Electrophoretic Deposition

Leonid V. Kovalev,[†] Marta V. Yarmolich,[†] Manuela L. Petrova,[‡] Jon Ustarroz,[‡] Herman A. Terryn,[‡] Nikolai A. Kalanda,[†] and Mikhail L. Zheludkevich*[,§,⊥]

[†]Scientific-Practical Materials Research Centre, NAS of Belarus, P. Brovka Street, 19, 220072 Minsk, Belarus

[‡]Research Group Electrochemical and Surface Engineering, Department of Materials and Chemistry, Vrije Universiteit Brussel, Pleinlaan 2, 1050 Brussel, Belgium

[§]Departamento de Engenharia de Materiais e Ceramica and CICECO, Universidade de Aveiro, 3810-193 Aveiro, Portugal

ABSTRACT: The present work reports on the new approach to create metal-supported Sr_2FeMoO_6 (SFMO)-based electrodes that have high potential to be applied in solid oxide fuel cells. The SFMO films were formed on stainless steel substrates by electrophoretic deposition (EPD) method. Ethyl alcohol with phosphate ester as a dispersant and isopropyl alcohol with I_2-acetone mixture as a charge additive were considered as an effective medium for EPD of SFMO particles. The synthesis of SFMO powder as well as suspension preparation and deposition kinetics were systematically studied. The effect of applied voltage on the thickness and morphology of SFMO films was established. The microstructure of the deposits was examined by electron microscopy. The thickness, morphology and porosity of the SFMO layers can be fine-tuned by varying solvent, charging additives, deposition time, and applied voltage. According to X-ray photoelectron spectroscopy analysis, it was found that Fe^{3+}–Mo^{5+} and Fe^{2+}–Mo^{6+} pairs coexist, whereas the valent balance shifts toward an Fe^{2+}–Mo^{6+} configuration.

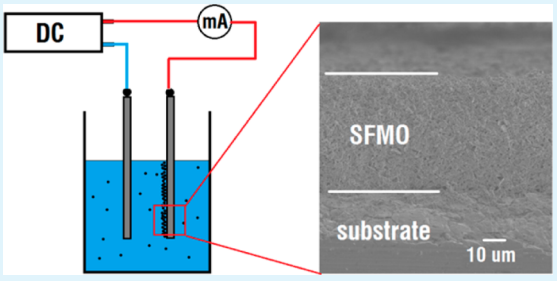

KEYWORDS: *double perovskite, electrophoretic deposition, solid oxide fuel cell, XPS analysis, magnetic films*

INTRODUCTION

The magnetic material Sr_2FeMoO_6 (SFMO) with a double perovskite structure has been widely investigated in the past decade due to a wide range of potential applications such as magnetic sensors, spin valves and magnetoresistive random-access memory (MRAM).[1] This is attributed to the unique properties of SFMO, such as practically 100% spin polarization of the conduction electrons, high Curie temperature (above 410 K), large values of low field magnetoresistance (up to 15% at B = 0.1 T, T = 4.2 K) and low values of operation magnetic fields.[2−5]

Moreover, recently a high potential of SFMO-based electrodes to be used as electrodes for solid oxide fuel cells (SOFCs) was demonstrated.[6−10] Hence, SFMO films are also of great interest for next-generation energy conversion devices.[11,12] Perovskite solid solutions in a mixed-valent state with oxygen deficiency are advanced materials used as anodes for SOFC due to their high ionic and electronic conductivity and good electrochemical activity in a reducing atmosphere.[6,8] Moreover, the possibility for SFMO fabrication with cation substitution ($Sr_2Fe_xMo_{1-x}O_6$) in a wide range triggers both the oxygen vacancies and the electronic defects, which allows obtaining electrodes with the desired properties.[7]

SOFC electrodes are typically fabricated by a screen-printing technique,[6,8] infiltration,[13] or self-combustion technique.[14] However, in view of a commercial application, electrophoretic deposition (EPD) is a more suitable method.[15] EPD is especially attractive to prepare SOFC electrodes due to its simplicity, cost-effectiveness and the possibility of engineering thick films on substrates with different shapes.

However, in spite of the growing interest of SFMO films and the fact that many different types of perovskite materials are widely used in the EPD process,[15−19] little work has been published on preparation of SFMO layers by EPD technique. Only very recently the magnetic and structural properties of SFMO films fabricated by EPD have been studied,[20] though without focusing on the EPD process. Alternatively, the present study aims at finding a suitable system solvent–dispersant, investigating EPD kinetics, optimizing deposition conditions and characterizing the obtained SFMO films.

EXPERIMENTAL SECTION

Powder Preparation. Powder of ferrimagnetic SFMO was prepared using the citrate–gel method.[21,22] Initially, aqueous solutions of $Sr(NO_3)_2$ (0.4 mol/L) and $Fe(NO_3)_3{\cdot}9H_2O$ (0.2 mol/L) were mixed in a mole ratio of 2:1 = n(Sr):n(Fe) with the addition of citric acid as a chelating agent. Then, an aqueous solution of $(NH_4)_6Mo_7O_{24}{\cdot}4H_2O$ (0.2 mol/L) was added in a mole ratio of 1:1 = n(Mo):n(Fe). Ethylendiamine was added to adjust the desired pH

Received: August 4, 2014
Accepted: October 3, 2014
Published: October 3, 2014

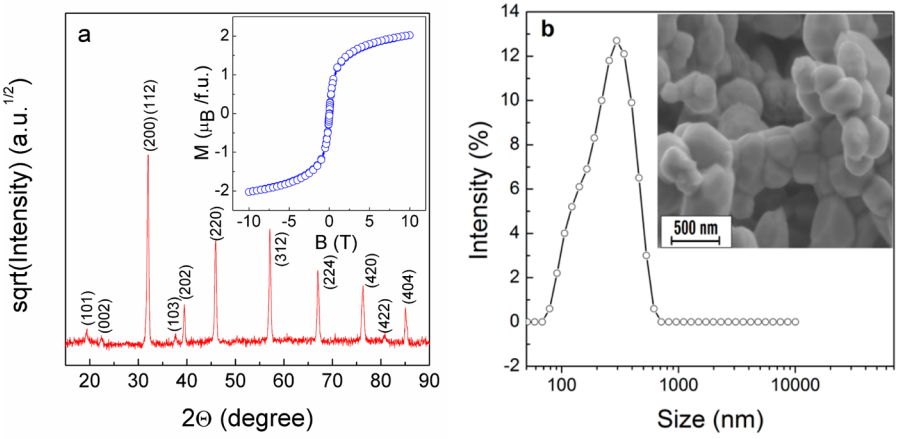

Figure 1. (a) XRD spectra of SFMO powder in square scale. Inset: magnetization hysteresis loop of SFMO powder recorded at 4.2 K. (b) Size destribution of SFMO particles synthesized by citrate−gel method measured by DLS in ethanol. Inset: FESEM image of SFMO powder.

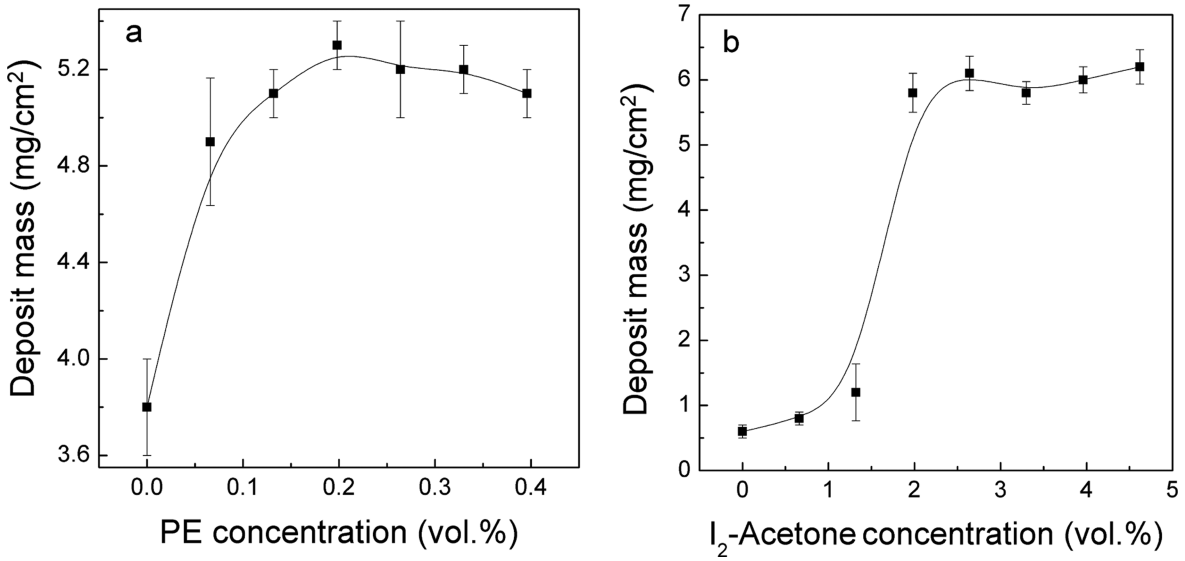

Figure 2. Mass of the deposited films as a function of the concentration of different additives. (a) Phosphate ester (PE) in a SFMO suspension in ethyl alcohol. (b) I_2−acetone mixture in a SFMO suspension in isopropyl alcohol. Deposition voltage U = 50 V and time t = 2 min.

value. The resulting solution was continuously stirred at 80 °C until a light green gel was formed. The obtained gel was dried in an oven at 200 °C to form a black solid foam. Then, the foam was ground in powder and preheated at 500 °C in air for 10 h. Finally, SFMO powder was prepared by annealing at 850 °C for 5 h in an Ar/H_2(5%) gas flow.

Suspension Preparation. The suspensions of pure SFMO particles were prepared in different solvents: deionized water, ethanol, isopropyl alcohol and a mixture of acetylacetone and ethanol with volume ratio of 1:1. The concentration of SFMO in all suspensions was 7 g/L. Phosphoric acid dibutyl ester (PE) and I_2 in acetone solution (6 g/L) were utilized as charge additives. The conductivity of the suspension was measured with a Lab 970 conductometer (Schott Instruments).

Electrophoretic Deposition. For EPD processes, conductive substrates are conventionally utilized. In this work, stainless steel plates were used. It must be noted that EPD is also possible on high resistive solid electrolyte substrates, by simply covering them with a metallic thin film.[19] A glass covered indium tin oxide (ITO) film was used as a counter electrode. The distance between the cathode and anode was 10 mm. The suspensions were treated in an ultrasonic bath during 20 min right before EPD. EPD experiments were performed at a constant voltage in a voltage range between 20 and 300 V using an Agilent N8742A DC power supply. To determine the mass of the deposit, substrates were weighted before and after the deposition, followed by drying at 50 °C for 5 h.

Characterization. The microstructure and morphology of both the powders and SFMO films were investigated using field emission scanning electron microscopy (FESEM, JEOL JSM-7000F). The phase composition and structural characterization of the samples were determined by X-ray diffraction (XRD) measurements with Cu Kα radiation using FullProf software. Particle size of the powders was measured by dynamic light scattering (DLS) on a Zetasizer Nano particles analyzer (Malvern Nano ZS90, U.K.). X-ray photoelectron spectroscopy (XPS) measurements were performed in a PHI 5600 (Physical Electronics) photoelectron spectrometer using the monochromatic Al Kα line 1486.6 eV at 350.0 W at a base pressure of $7.5 \cdot 10^{-10}$ Torr at 48.95 eV pass energy. The energy scale was calibrated according to ISO 15472 standard. The analytical surface was 800 μm^2. The angle between analyzer and sample surface was 45°.

RESULTS AND DISCUSSION

Powder Characterization. According to XRD data, synthesized powder of SFMO had a tetragonal perovskite structure without any impurities (Figure 1a). Rietveld profile analysis was performed in $I4/mmm$ space group, and the cell parameters were defined as $a = b = 0.557$ nm, $c = 0.789$ nm.

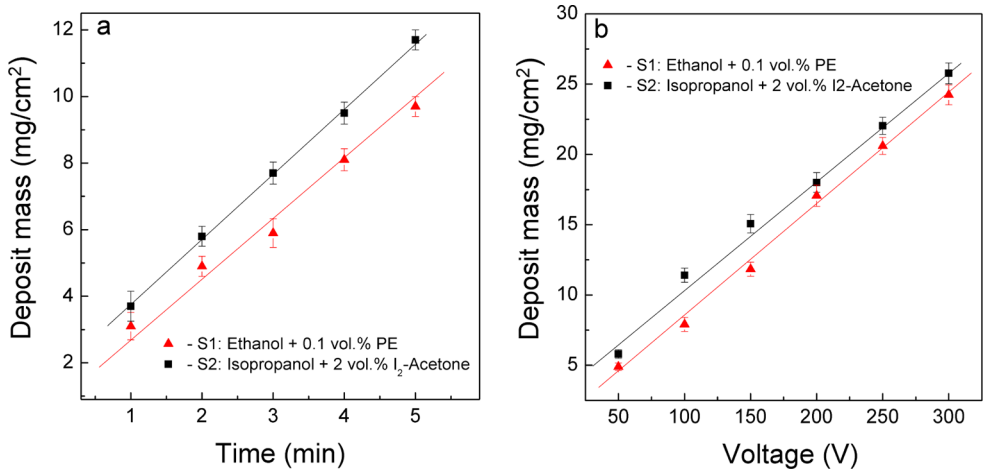

Figure 3. (a) Mass of the deposited films as a function of deposition time at constant voltage 50 V. (b) Mass of the deposited films as a function of the applied voltage at constant deposition time of 2 min.

The degree of antisite defects (ASD) was 15%. The magnetization hysteresis loop recorded at 4.2 K, reported in the inset of Figure 1a, displays a typical ferromagnetic behavior with a small coercivity and is not saturated at the magnetic field 10 T. The reason for the nonsaturation of hysteresis loop is the presence of antisite defects, that leads to long-range magnetic ordering destruction and origin of frustrated magnetic states. Figure 1b shows the size destribution of SFMO particles measured in ethanol by DLS. The average particle size was around 300 nm, in a good agreement with FESEM data (inset of Figure 1b).

EPD and Film Characterization. It is well-known that one of the important steps of EPD is the preparation of stable and well-dispersed suspensions, which requires a suitable solvent.[23,24] Therefore, a series of the following solvents were tested in the present work: deionized water, ethanol, isopropyl alcohol and a mixture of acetylacetone and ethanol with volume ratio of 1:1. Moreover, a suitable dispersant or a charge additive was added at an appropriate concentration to obtain the suspension of desirable stability with tuned electrophoretic mobility.

The SFMO suspensions prepared in the mixture of acetylacetone and ethanol showed low stability with a fast sedimentation. Adding an I_2−acetone mixture as a charge additive did not improve the stability, and finally, a noticeable deposition was not obtained. That being the case, further experiments did not use this solvent.

It was observed that SFMO powders dispersed in aqueous solvents were completely decomposed into Fe_2O_3 (hematite), $SrMoO_4$ and $SrCO_3$ phases under ultrasonic treatment. Recently, it was also reported that SFMO reacts with water at temperatures above 100 °C.[7] It could be concluded that SFMO is unstable in water. Hence, aqueous solvents are not suitable for EPD of SFMO particles.

SFMO suspensions in pure ethanol showed good stability and cathodic deposition was possible. However, the deposits obtained in pure ethanol were highly agglomerated and nonuniform. Therefore, phosphate ester (PE) was used to improve the quality of the deposited films. It must be noted that PE is an effective electrostatic stabilizer, which positively charges the particles in ethanol by donating protons to the particle surface.[15,23] Increasing PE concentration in the suspensions up to 0.2 vol % increases the deposition rate (Figure 2a), which indicates an increase of the particles charge. However, further increasing PE content in the suspension leads to a slow decrease of the deposition rate.

Cathodic deposits were also obtained from the SFMO suspension in pure isopropyl alcohol. However, the deposition rate was almost 10 times lower in comparison with the deposition rate in pure ethanol suspensions. To increase the deposition rate, an I_2−acetone mixture was added to the isopropyl alcohol suspensions. A mixture of acetone and iodine was perceived as an effective charge additive.[23,25] Particle charging can be achieved via proton adsorption, activated by the keto−enol reaction and catalyzed by I_2, as reported elsewhere.[23,24] Figure 2b shows the deposit mass of SFMO versus the concentration of I_2−acetone additive. It can be seen that the deposition rate rapidly increases in the concentration range 1−2 vol %, but then the deposition rate is almost constant when further increasing the charge additive concentration.

A key aspect to achieve successful EPD is particle mobility. In this context, it is important to tune the experimental conditions to obtain high electrophoretic mobility while the ionic conductivity of the suspension remains low.[19,24,26] For this reason, to carry out the optimization of deposition conditions, the authors chose two suspensions of SFMO, which are denoted henceforward as S1 and S2. These are SFMO suspensions in ethanol with 0.1 vol % PE and in isopropyl alcohol with 2 vol % I_2−acetone mixture, respectively. The additive concentration values in suspensions S1 and S2 correspond to the case of the largest deposition rate for the least ionic conductivity of suspensions (2.2 and 0.2 μS/cm for S1 and S2, respectively).

The SFMO deposit mass increases almost linearly with increasing the deposition time for both S1 and S2 suspensions, as shown in Figure 3a. This fact indicates that the film thickness can be accurately tuned using different durations of the process. Another parameter that can be potentially used to control the deposition process is voltage. The mass of SFMO deposits as a function of the applied voltage for suspensions S1 and S2 is plotted in Figure 3b. Approximately a linear relationship between the deposit mass (m) and the applied voltage was observed in a voltage range from 50 to 300 V for both suspensions, as predicted by the Hamaker's law:[27]

$$m = \mu CEt \quad (1)$$

where μ is the electrophoretic mobility, C is the concentration of particles in suspension, E is the electric field strength, $E = V/d$, where V is the applied voltage, d is the distance between electrodes and t is the deposition time.

In spite of the fact that deposition kinetics linearly depends on the applied voltage and higher rates can be achieved, the uniformity of the layer can be negatively affected when too high of voltages are used. The deposited films were highly nonuniform, when the applied voltage was higher than 150 V (Figure 4a). In comparison, Figure 4b presents the deposited

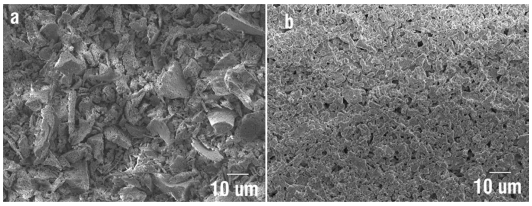

Figure 4. Typical FESEM images of SFMO films obtained at deposition voltages of (a) 150 V and (b) 50 V for suspension S1 (solvent: ethyl alcohol, with 0.1 vol % PE) at a deposition time of 1 min.

films obtained at 50 V. In the case of high voltages (>150 V), many agglomerates with average dimensions up to 50 μm were formed on the deposit surface, as it has been observed previously.[28,29] Moreover, the solvent turbulence at high voltages can also be a cause of nonuniform deposition.[24,30,31] Decrease of the deposition voltage below 50 V leads to even better quality of the layer.

The interplay between the deposition time and the applied voltage allows us to fine-tune the morphology and the thickness of SFMO EPD layers. The highest uniformity of the film is obtained at low deposition voltages. The desired thickness of the deposit can be achieved by increasing the deposition time. On the basis of these observations, the optimization of the deposition conditions was carried out and deposits of the best quality were obtained at a low voltage of 20 V and a deposition time of 10 min. Figure 5 shows typical FESEM images of both the surface and cross-section of SFMO films deposited from S1

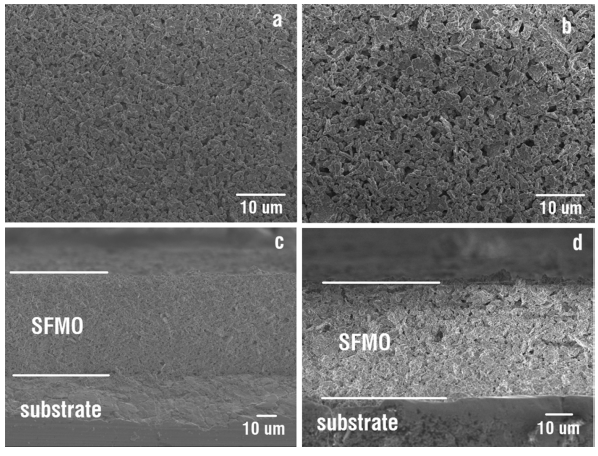

Figure 5. FESEM images of films obtained from SFMO suspensions (a) S1 (solvent: ethanol, with 0.1 vol % PE) and (b) S2 (solvent: isopropyl alcohol, with 2 vol % I_2–acetone mixture), at a deposition voltage of 20 V and time of 10 min. (c, d) Cross-section images of deposits from S1 and S2, respectively.

and S2 suspensions under optimized deposition conditions. The deposits were uniform and crack-free for both series of films. However, the porosity of the films prepared from the S2 suspension was noticeably higher than in the case of films obtained from the S1 suspension. Analysis of FESEM cross-section images of the films prepared at different deposition durations showed that the deposit thickness can be varied in the range of 10–60 μm by the varying the deposition time, which is in agreement with the results shown in Figure 3a.

Figure 6 shows XRD spectra of SFMO films obtained from S1 and S2 suspensions under optimized deposition conditions:

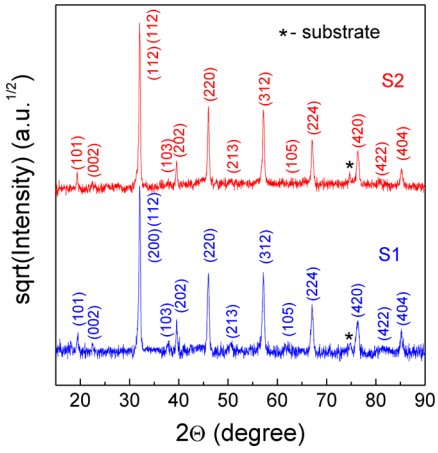

Figure 6. XRD spectra of SFMO films deposited from S1 (solvent: ethanol, with 0.1 vol % PE) and S2 (solvent: isopropyl alcohol, with 2 vol % I_2–acetone mixture) suspensions at a deposition voltage of 20 V and a time of 10 min. Intensity in square scale.

voltage 20 V and time 10 min. According to Rietveld full profile analysis of XRD data, the samples of both series were single phase and had tetragonal structure ($I/4mmm$) with super structural ordering of the Fe and Mo cations. The crystal lattice parameters were approximately equal for both films, deposited from S1 and S2 suspensions and have been calculated as $a = b =$ 0.557 nm, $c = 0.79$ nm and $V = 0.245$ nm^3. ASD amounted to 16% and 19% for S1 and S2, respectively.

The chemical states of Fe and Mo elements in the SFMO films were determined from XPS data. It is evident from Figure 7a that the Fe 2p XPS spectra of the investigated films consist of Fe $2p_{3/2}$ and Fe $2p_{1/2}$ excitations. Mo 3d XPS spectra (Figure 7b) show two peaks from Mo $3d_{5/2}$ and Mo $3d_{3/2}$ excitations. In addition, no signs of impurity phases of Fe^0 and Mo^{4+} species were detected in the investigated films, in good agreement with XRD data. The mixed valent state was evaluated by curve fitting of the Fe 2p and Mo 3d core-level spectra (Figure 7).

The binding energies were calibrated, referred to the C 1s peak from carbon contamination of the samples at 284.9 eV to correct for charging effects. The PHI Multipack 9.3 software was used for data interpretation. The Mo 3d peak was fitted by using four components, two for the $3d_{3/2}$ and two for the $3d_{5/2}$, indicating the Mo^{5+} and Mo^{6+} valence states, respectively. The distance between doublets was taken as 3.13 eV and the (Mo $3d_{5/2}$):(Mo $3d_{3/2}$) area ratio was fixed to be equal to 3:2. A similar situation was with Fe 2p peak fitting, two components for the $2p_{3/2}$ and two for the $2p_{1/2}$, indicating the Fe^{3+} and Fe^{2+} valence states, respectively. The distance between doublets was taken as 13.6 eV and the (Fe $2p_{3/2}$):(Fe $2p_{1/2}$) area ratio was

dx.doi.org/10.1021/am5052125 | ACS Appl. Mater. Interfaces 2014, 6, 19201–19206

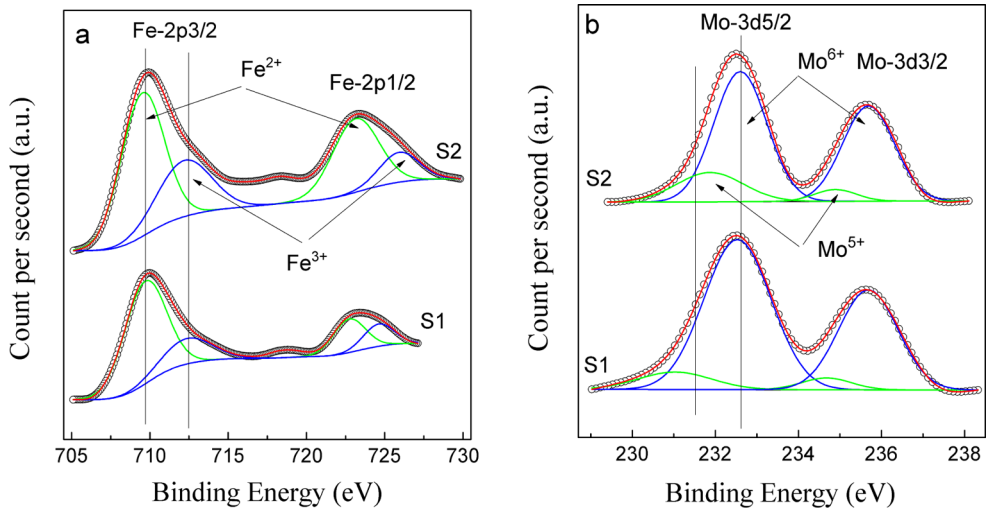

Figure 7. Fe 2p (a) and Mo 3d (b) core-level spectra of SFMO films obtained from S1 (solvent: ethyl alcohol, with 0.1 vol % PE) and S2 (solvent: isopropyl alcohol, with 2 vol % I_2–acetone mixture) suspensions at a deposition voltage of 20 V and a time of 10 min.

fixed to be equal to 2:1.[32] The binding energies and the percentage contributions of the valent states of Fe and Mo in the investigated films are summarized in Table 1.

Table 1. Binding Energies and Percentage Contributions of Core Electrons of SFMO Film Deposited from the S1 and S2 Suspensions

	Mo $3d_{5/2}$		Fe $2p_{3/2}$	
	Mo^{6+} (%)	Mo^{5+} (%)	Fe^{2+} (%)	Fe^{3+} (%)
S1	232.35 (81%)	230.50 (19%)	709.82 (78%)	712.55 (22%)
S2	232.60 (76%)	231.87 (24%)	709.52 (72%)	712.20 (28%)

The valent balance of Fe^{2+}/Fe^{3+} and Mo^{5+}/Mo^{6+} cations was shifted to Fe^{2+}–Mo^{6+} configuration for both samples. Similar results have been previously observed.[6,9] In these cases, it was shown that the existence of a mixed valent state plays an important role in the formation of metallic electronic conduction by degeneracy and hybridization of Fe^{2+}–Mo^{6+} and Fe^{3+}–Mo^{5+} couples and increasing of the degree of valence degeneracy results in enhanced metallic behavior. The Fe^{2+}–Mo^{6+}/Fe^{3+}–Mo^{5+} couples are suggested to generate electronic carriers, as well as to introduce oxygen vacancies into the lattice to allow ionic conduction and situations where mixed ionic and electronic conduction occur.[33] For this reason, SFMO has great advantages in applications as both an anode and cathode in symmetrical SOFCs.

CONCLUSON

The SFMO films with tunable thickness and porosity were formed on metallic electrodes using a water free electrophoretic deposition method. EPD was performed using a submicrometer ceramic powder of Sr_2FeMoO_6 prepared by a citrate–gel method and dispersed in ethyl alcohol with phosphate ester as a dispersant or alternatively in isopropyl alcohol with an I_2–acetone mixture as a charge additive.

Deposited films were single phase with a super structural ordering of Fe and Mo cations. Absence of impurity phases indicates that SFMO powder does not degrade in the selected solvent–dispersant systems. Films deposited from the ethyl alcohol–phosphate ester system were more uniform and had higher density compared with the films deposited from the isopropyl alcohol–(I_2–acetone) system. Thus, the film porosity can be varied by choosing the appropriate solvent–dispersant system, which is important in view of their applications.

It has been shown that electrophoretic deposition follows Hamaker's law; therefore, film thickness can be accurately controlled by adjusting deposition parameters such as deposition time, voltage and suspension concentration. The EPD process performed at lower voltages leads to more uniform dense layers of SFMO. The use of voltages higher than 150 V causes particle agglomeration and solution turbulence, leading to nonuniform deposits.

Coexistence of Fe^{3+}–Mo^{5+} and Fe^{2+}–Mo^{6+} pairs was proved, together with a shift of the valent balance toward the Fe^{2+}–Mo^{6+} configuration. The existence of mixed valent states plays an important role in the formation of metallic electronic conduction by degeneracy and hybridization of Fe^{2+}–Mo^{6+} and Fe^{3+}–Mo^{5+} couples. Increasing the degree of valence degeneracy results in enhanced metallic behavior and generates a situation in which mixed ionic and electronic conduction occur. Therefore, films of double perovskite Sr_2FeMoO_6 fabricated by EPD have great potential to be used both as an anode and cathode in SOFCs.

AUTHOR INFORMATION

Corresponding Author

*M. L. Zheludkevich. E-mail: mzheludkevich@ua.pt.

Present Address

[⊥]Institute of Materials Research, Helmholtz-Zentrum Geesthacht, 21502 Geesthacht, Germany

Notes

The authors declare no competing financial interest.

ACKNOWLEDGMENTS

The work has been supported by the 7th FWP NANEL project PIRSES-GA-2011-295273.

REFERENCES

(1) Serrate, D.; Teresa, J.; Ibarra, M. Double Perovskites with Ferromagnetism above Room Temperature. *J. Phys.: Condens. Matter* **2007**, *19*, 023201–023287.

(2) Huang, Y.; Yamauchi, H.; Karppinen, M. Large Low-Field Magnetoresistance Effect in Sr_2FeMoO_6 Homocomposites. *Appl. Phys. Lett.* **2005**, *86*, 0725101−0725103.
(3) Kanchana, V.; Vaitheeswaran, G.; Alouani, M.; Delin, A. Electronic Structure and X-ray Magnetic Circular Dichroism of Sr_2FeMoO_6: Ab Initio Calculations. *Phys. Rev. B* **2007**, *75*, 220404−2204044.
(4) Chmaissem, O.; Kruk, R.; Dabrowski, B.; Brown, D.; Xiong, X.; Kolesnik, S.; Jorgensen, J.; Kimball, C. Structural Phase Transition and the Electronic and Magnetic Properties of Sr_2FeMoO_6. *Phys. Rev. B* **2000**, *6*, 14197−14206.
(5) Kalanda, N.; Kovalev, L.; Zheludkevich, M.; Garamus, V.; Willumeit, R.; Sobolev, N. Charge Transfer Processes and Magneto-resistance in Strontium Ferromolybdate with Dielectric Barriers. *Phys. Status Solidi B* **2013**, *250*, 825−830.
(6) Wang, Z.; Tian, Y.; Li, Y. Direct CH_4 Fuel Cell Using Sr_2FeMoO_6 as an Anode Material. *J. Power Sources* **2011**, *196*, 6104−6109.
(7) Wright, J.; Virkar, A.; Liu, Q.; Chen, F. Electrical Characterization and Water Sensitivity of $Sr_2Fe_{1.5}Mo_{0.5}O_6$ À d as a Possible Solid Oxide Fuel Cell Electrode. *J. Power Sources* **2013**, *237*, 13−18.
(8) Liu, Q.; Bugaris, D.; Xiao, G.; Chmara, M.; Ma, S.; Loye, H.; Amiridis, M.; Chen, F. $Sr_2Fe_{1.5}Mo_{0.5}O_{6-\delta}$ as a Regenerative Anode for Solid Oxide Fuel Cells. *J. Power Sources* **2011**, *196*, 9148−9153.
(9) Zhang, L.; Zhou, Q.; He, Q.; He, T. Double-Perovskites $A_2FeMoO_{6-\delta}$ (A=Ca, Sr, Ba) as Anodes for Solid Oxide Fuel Cells. *J. Power Sources* **2010**, *195*, 6356−6366.
(10) Suthirakun, S.; Ammal, S.; Ana, B.; García, M.; Xiao, G.; Chen, F.; Loye, H.; Carter, K.; Heyden, A. Theoretical Investigation of H_2 Oxidation on the $Sr_2Fe_{1.5}Mo_{0.5}O_6$ (001) Perovskite Surface under Anodic Solid Oxide Fuel Cell Conditions. *J. Am. Chem. Soc.* **2014**, *136*, 8374−8386.
(11) Jacobson, A. Materials for Solid Oxide Fuel Cells. *Chem. Mater.* **2010**, *22*, 660−674.
(12) Tietz, F.; Buchkremer, H.; Sto, D. Components Manufacturing for Solid Oxide Fuel Cells. *Solid State Ionics* **2002**, *152*, 373−381.
(13) Meng, X.; Han, D.; Wu, H.; Li, J.; Zhan, Z. Characterization of $SrFe_{0.75}Mo_{0.25}O_{3-\delta}$−$La_{0.9}Sr_{0.1}Ga_{0.8}Mg_{0.2}O_{3-\delta}$ Composite Cathodes Prepared by Infiltration. *J. Power Sources* **2014**, *246*, 906−911.
(14) Dai, N.; Wang, Z.; Lou, Z.; Yan, Y.; Qiao, J.; Peng, J.; Sun, K. One-Step Synthesis of High Performance $Sr_2Fe_{1.5}Mo_{0.5}O_6$−$Sm_{0.2}Ce_{0.8}O_{1.9}$ Composite Cathode for Intermediate-Temperature Solid Oxide Fuel Cells Using a Self-Combustion Technique. *J. Power Sources* **2012**, *217*, 519−523.
(15) Zhitomirsky, I.; Petric, A. Electrophoretic Deposition of Ceramic Materials for Fuel Cell Applications. *J. Eur. Ceram. Soc.* **2000**, *20*, 2055−2061.
(16) Jian, G.; Zhou, D.; Yang, J.; Shao, H.; Xue, F.; Fu, Q. Microstructure and Multiferroic Properties of $BaTiO_3/CoFe_2O_4$ Films on Al_2O_3/Pt Substrates Fabricated by Electrophoretic Deposition. *J. Eur. Ceram. Soc.* **2013**, *33*, 1155−1163.
(17) Zhou, D.; Jian, G.; Zheng, Y.; Gong, S.; Shi, F. Electrophoretic Deposition of $BaTiO_3/CoFe_2O_4$ Multiferroic Composite Films. *Appl. Surf. Sci.* **2011**, *257*, 7621−7626.
(18) Ma, J.; Cheng, W. Deposition and Packing Study of Sub-Micron PZT Ceramics Using Electrophoretic Deposition. *Mater. Lett.* **2002**, *56*, 721−727.
(19) Ponzoni, C.; Rosa, R.; Cannio, M.; Buscaglia, V.; Finocchio, E.; Nanni, P.; Leonelli, C. Electrophoretic Deposition of Multiferroic $BiFeO_3$ Sub-Micrometric Particles from Stabilized Suspensions. *J. Eur. Ceram Soc.* **2013**, *33*, 1325−1333.
(20) Zhang, Q.; Xu, Z.; Liang, J.; Pei, J.; Sun, H. Structural and Magnetic Properties of Sr_2FeMoO_6 Film Prepared by Electrophoresis Technique. *J. Magn. Magn. Mater.* **2014**, *354*, 231−234.
(21) Suominen, T.; Raittila, J.; Salminen, T.; Schlesier, K.; Lindén, J.; Paturi, P. Magnetic Properties of Fine SFMO Particles: Super-paramagnetism. *J. Magn Magn Mater.* **2007**, *309*, 278−284.
(22) Santillán, M.; Caneiro, A.; Quaranta, N.; Boccaccini, A. Electrophoretic Deposition of $La_{0.6}Sr_{0\cdot4}Co_{0.8}Fe_{0.2}O_{3-\delta}$ Cathodes on $Ce_{0.9}Gd_{0.1}O_{1.95}$ Substrates for Intermediate Temperature Solid Oxide Fuel Cell (IT-SOFC). *J. Eur. Ceram Soc.* **2009**, *29*, 1125−1132.
(23) Zhitomirsky, I. Cathodic Electrodeposition of Ceramic and Organoceramic Materials. Fundamental Aspects. *Adv. Colloid Interface Sci.* **2002**, *97*, 279−317.
(24) Besra, L.; Liu, M. A Review on Fundamentals and Applications of Electrophoretic Deposition (EPD). *Prog. Mater. Sci.* **2007**, *52*, 1−61.
(25) Fori, B.; Taberna, P.; Arurault, L.; Bonino, J.; Gazeau, C.; Bares, P. Electrophoretic Impregnation of Porous Anodic Aluminum Oxide Film by Silica Nanoparticles. *Colloids Surf.* **2012**, *415*, 187−194.
(26) Corni, I.; Ryan, M.; Boccaccini, A. Electrophoretic Deposition: From Traditional Ceramics to Nanotechnology. *J. Eur. Ceram. Soc.* **2008**, *28*, 1353−1367.
(27) Hamaker, H. Formation of Deposition by Electrophoresis. *Trans. Faraday Soc.* **1940**, *36*, 279−283.
(28) Zhitomirsky, I. Cathodic Electrophoretic Deposition of Diamond Particles. *Mater. Lett.* **1998**, *37*, 72−78.
(29) Zhitomirsky, I.; Gal-Or, L. Electrophoretic Deposition of Hydroxyapatite. *J. Mater. Sci.: Mater. Med.* **1997**, *8*, 213−219.
(30) Maleki-Ghaleh, H.; Rekabeslami, M.; Shakeri, M.; Siadati, M.; Javidi, M.; Talebian, S.; Aghajani, H. Nano-Structured Yttria-Stabilized Zirconia Coating by Electrophoretic Deposition. *Appl. Surf. Sci.* **2013**, *280*, 666−672.
(31) Negishi, H.; Yamaji, K.; Sakai, N.; Horita, T.; Yanagishita, H.; Yokokawa, H. Electrodeposition of YSZ Powders for Solid Oxide Fuel Cells. *J. Mater. Sci.* **2004**, *39*, 833838−833845.
(32) Wagner, C.; Moulder, J.; Muilenberg, G.; Chastain, J.. *Handbook of X-ray Potoelectron Spectroscopy: A Reference Book of Standard Data for Use in X-ray Photoelectron Spectroscopy*; Physical Electronics Division, Perkin-Elmer Corp.: Eden Prairie, MN, 1979; p 261.
(33) Xiao, G.; Liu, Q.; Zhao, F.; Zhang, L.; Xia, C. $Sr_2Fe_{1.5}Mo_{0.5}O_6$ as Cathodes for Intermediate-Temperature Solid Oxide Fuel Cells with $La_{0.8}Sr_{0.2}Ga_{0.87}Mg_{0.13}O_3$ Electrolyte. *J. Electrochem. Soc.* **2011**, *158*, 455−460.